Scanning-tunneling-microscopy studies of (2×3)N-induced structures, thermal desorption, and oxygen coadsorption on the Cu{110} surface

F. M. Leibsle, R. Davis,* and A. W. Robinson
Interdisciplinary Research Centre in Surface Science, University of Liverpool, Liverpool L69 3BX, United Kingdom
(Received 15 June 1993; revised manuscript received 29 November 1993)

We have used scanning tunneling microscopy (STM) to investigate (2×3)N-induced structures arising from the bombardment of activated nitrogen onto the Cu{110} surface followed by annealing. We have examined these structures for a variety of nitrogen doses, beam energies, and annealing temperatures. Increasing the nitrogen dose resulted in the gradual appearance of an additional N-induced structure also possessing a (2×3) periodicity. Studies were performed on various desorption mechanisms (thermal and tip induced). Images of the surface after heating to temperatures at which partial desorption of the (2×3)N reconstruction occurred show that thermal desorption results in islands of clean Cu centered on step edges. Pulsing the voltage between the sample and tunneling tip was also found to induce desorption. We have formed codomains of the (2×1)O and (2×3)N reconstructions. Images of the codomains yield the registry of features within the (2×3)N reconstructions with respect to the substrate and suggest a double added row mechanism for the formation of the (2×3)N reconstruction. Models are presented for both the (2×3)N-induced structures.

I. INTRODUCTION

The Cu{110}-(2×3)N system has been studied with a variety of techniques in recent years but with very little agreement between experimental results. This system was studied by Heskett, Baddorf, and Plummer using thermal-desorption spectroscopy (TDS), low-energy electron diffraction (LEED), and high-resolution electron-energy-loss spectroscopy (HREELS).[1] In that study atomic nitrogen was deposited by using an ion gun to bombard the clean surface. After nitrogen deposition followed by annealing to 600 K a (2×3) LEED pattern was reported. HREELS measurements suggested that the N atoms occupy long-bridge sites. Baddorf and Zehner studied this system with LEED, TDS, x-ray photoelectron spectroscopy (XPS), and Auger-electron spectroscopy (AES).[2] Their LEED and TDS results agreed well with the previous study except that their thermal-desorption line shapes differed somewhat. From their XPS measurements, they concluded that $\frac{2}{3}$ of a monolayer of N atoms were involved in the (2×3)N reconstruction. Other studies have been performed to determine the surface structure of the (2×3)N reconstruction. A photoelectron-diffraction study[3] was unable to differentiate between adsorption in the long-bridge site and in the fourfold-hollow site. A low-energy ion-scattering study, which indicated a contraction of the lattice spacing in the [001] direction,[4] led to the proposal of a pseudosquare reconstruction, which is essentially a Cu{100}-c(2×2)N layer superimposed over the Cu{110} surface.[3–5] A subsequent low-energy ion-scattering study by Spitzl, Niehus, and Comsa contradicted these results.[6] In this study, no change was observed in the periodicity of the Cu atoms in the [1$\bar{1}$0] direction, from which it was concluded that it is the arrangement of the nitrogen atoms in the (2×3) reconstruction that is responsible for the doubling of periodicity in this direction. These measurements further suggested that every third ⟨110⟩ close-packed row of the outermost Cu layer was missing. Coupled with an Auger-electron spectroscopy measurement for the N coverage of 0.2±0.05 ML, a missing-row model was proposed in which every third ⟨110⟩ row of Cu atoms was missing, with N atoms located in long-bridge sites between every other pair of Cu atoms within the remaining rows. This requires a nitrogen coverage of $\frac{1}{6}$ of a monolayer, in strong contrast to the 0.63-ML measurement of Baddorf and Zehner.[2] An early scanning-tunneling-microscopy (STM) study was interpreted to be consistent with this structural model;[7] however, a subsequent STM study observed additional features which question the positioning of the nitrogen atoms within the missing-row model and showed a dependency on the surface structure as a function of the nitrogen dose, suggesting the existence of high- and low-nitrogen-coverage (2×3) reconstructions.[8] A recent analysis of LEED I-V curves could not produce strong support for the model proposed in Refs. 6 and 7, nor did it provide strong support for any of the previously proposed models. In fact, a structural model with missing rows of Cu atoms running in the [001] direction, orthogonal to the missing-row model proposed earlier,[6,7] gave best agreement between experimental results and theoretical simulations for an extensive set of possible surface reconstructions.[9]

In this study, we summarize our attempts to understand the Cu{110}-(2×3)N system via the use of scanning tunneling microscopy. We have performed detailed studies on the nitrogen-coverage dependence of the surface to see how the (2×3) structures form. We have looked at mechanisms by which the (2×3) reconstruction is removed from the surface, namely thermal and tip-induced desorption. We have coadsorbed oxygen to

view the relationship between codomains of (2×3) reconstructions and the well-understood (2×1)O reconstruction. This multifaceted approach has led us to propose structural models for both the (2×3)N reconstructions and to the realization that these structures are formed by added rows of Cu atoms.

II. EXPERIMENTAL DETAILS

These experiments were performed in an ultrahigh-vacuum chamber with a base pressure of 5×10^{-11} mbar. The STM used in this study was a commercial Omicron Vacuumphysik STM. The chamber also contained facilities for sample bombardment, LEED, and a quadrupole mass analyzer. The sample was mounted on a Ta baseplate with Ta clips. Sample heating was accomplished by electron-beam bombardment with the electrons striking the back of the baseplate. Sample temperatures were monitored by means of a Chromel-Alumel thermocouple mounted on the sample manipulator approximately 2 cm away from the sample. The Cu{110} surface (5×7 mm^2) was prepared by mechanical and electrochemical polishing and cleaned *in vacuo* by repeated cycles of argon-ion bombardment and annealing to 720 K until a sharp (1×1) pattern was observed by LEED. The nitride overlayers were prepared by ion bombardment of the crystal at room temperature for various lengths of time using 3.6×10^{-4} mbar of 99.999% purity N_2 and beam energies of either 500 or 200 eV. The typical ion current was approximately 5 μA. It should be pointed out that the current measured represents the nitrogen-ion flux incident on everything in electrical contact with the sample and not just the sample itself, hence the total integrated currents serve only as upper bounds for the actual nitrogen doses. Heating the crystal after nitrogen deposition to 600 K produced sharp (2×3) LEED patterns with low background intensities. Oxygen coadsorption studies were performed by backfilling the vacuum chamber to a pressure of 5×10^{-8} mbar of 99.999% purity oxygen for prescribed lengths of time.

III. DEPOSITION-DEPENDENT RESULTS

In our earlier study of this system,[8] we demonstrated that for very low N doses (typically on the order of 50 μC) followed by annealing to 600 K, the (2×3)N structures would form in rectangular islands elongated in the [1$\bar{1}$0] direction. This was surprising in that HREELS measurements suggest that both O and N bond in long-bridge sites on this surface.[1] Yet, the adsorption of oxygen results in a (2×1) reconstruction displaying island growth in the [001] direction.[10–15]

It was also observed that increasing the N dose resulted in the gradual appearance of an additional N-induced structure also possessing a (2×3) periodicity. Figures 1(a) and 1(b) show high-resolution images of both (2×3) N-induced structures. Three distinct atomic-scale features can be observed in these images. In Fig. 1(a), we observe the occasional presence of an atomic feature labeled *A* in the figure. The position of this *A* feature is directly in the center of four *B* features. Also, an additional periodic feature appears in the dark row separating the *B* features. We have designated this as feature *C*. In Fig. 1(b), which shows an image of a typical area of the surface after a much higher N dose using higher ion energy, the density of the *A* features is greatly increased. Although the tunneling conditions are considerably different for the two images, we found that the bias voltages and tunneling currents required to obtain atomic resolution varied considerably with the different tungsten

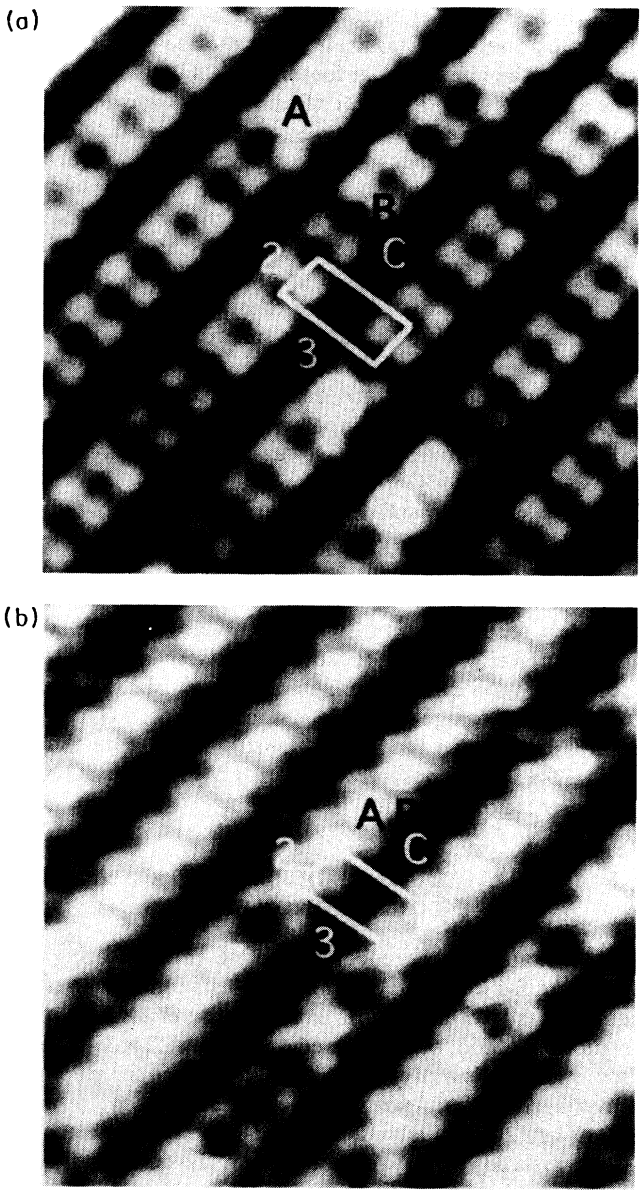

FIG. 1. (a) 60×60 Å^2 STM image of a typical area of the Cu{110} surface following a 200-eV 150-μC, N-ion bombardment and annealing to 600 K. (Sample bias −1.0 V, I=1 nA.) (b) 60×60 Å^2 STM image of a typical area of the Cu{110} surface following a 500-eV, 4400-μC, N-ion bombardment and annealing to 600 K. (Sample bias 0.06 V, I = 1 nA.) Atomic-scale features observed in these images are labeled *A*, *B*, and *C*. (2×3) unit cells are outlined. The only difference between the two images appears to be the increase in density of the *A* features.

tips used during the course of these studies. Once a particular set of tunneling parameters was found that yielded atomic resolution, however, the images obtained were quite reproducible.

We observed the following behavior in the surface density of the A features. For the subsaturation doses of 45 and 55 μC and the near-saturation dose of 150 μC, the density of A features remained constant at 0.25 A features per (2×3) unit cell. For a 450-μC dose at 200 eV followed by annealing to 600 K, the density rose to 0.58 A features per unit cell. A dose of 4800 μC, followed by the 600-K anneal, only resulted in a slight increase in the density of A features to 0.60 per (2×3) cell. We also explored the effect of ion energy on the resultant surface structure. Our results were consistent with that of Ref. 7, in that using beam energies of 500 eV created more damage on the surface resulting in a higher step density. However, we observed that the bombardment of 500-eV ions was more efficient in increasing the density of A features on the surface. For example, a 50-μC dose at 500 eV resulted in islands like those previously observed in Ref. 8, but within the islands the density of A features rose to 0.54 per unit cell. Likewise, a 4400-μC dose [Fig. 1(b)] resulted in a surface density of 0.8 A features per (2×3) unit cell. No attempt was made to study the effect of a 2-keV bombardment as was used in the low-energy ion-scattering study of Ref. 4.

That the density of the A features increased with increased nitrogen dosage and higher ion energies suggests that feature A is nitrogen derived. This was viewed as evidence for the existence of low- and high-coverage (2×3)N reconstructions, with the images of Fig. 1(a) and those of Ref. 7 being those of a low-coverage (2×3)N reconstruction and the images like Fig. 1(b) being those of a high-coverage (2×3)N reconstruction.[8] To further discuss these two reconstructions, we designate these as the $\alpha(2\times3)$N reconstruction [Fig. 1(a)] and the $\beta(2\times3)$N reconstruction [Fig. 1(b)].

IV. TEMPERATURE-DEPENDENT RESULTS AND DESORPTION STUDIES

We examined the effect of raising the annealing temperature for both the (2×3)N reconstructions. We were curious as to whether, for example, the $\alpha(2\times3)$N reconstruction could be converted into the $\beta(2\times3)$N reconstruction by simply annealing at higher temperatures. Prolonged annealing at 660 K of a surface containing rectangular (2×3)N islands resulted in a coalescence of the (2×3) islands but not an increase in the density of the A features. Likewise, further annealing of the $\beta(2\times3)$N reconstruction did not result in conversion to the $\alpha(2\times3)$N reconstruction or in an increase in the density of A features.

We also sought to raise the annealing temperatures to those at which we could expect partial desorption of the overlayer to occur and then reimage the surface in order to gain insight into the desorption process. We performed this phase of our experiments on a $\beta(2\times3)$N surface generated by 4400-μC nitrogen bombardment of the crystal at room temperature using a beam energy of 500 eV. Heating the crystal after nitrogen deposition to 600 K produced a sharp (2×3) LEED pattern with a low background intensity. After initial images were taken to check that we could resolve the $\beta(2\times3)$N reconstruction and assess the surface quality, the sample was then placed back into the sample manipulator and heated in 20- or 10-K temperature increments starting at 670 K. The sample was allowed to cool and then reimaged. Typically, the sample could be removed from the STM, heated, allowed to cool, and reinserted into the STM in 1 h time. Initially these temperature treatments had the effect of annealing the sample and resulted in a lower density of atomic steps. We discovered the first instances of thermal desorption, however, after the sample was heated to 690 K. We saw small areas in our images which appeared featureless, in contrast to the noticeable (2×3)N rows nearby. We interpret these areas to be clean areas of (1×1). Figure 2 shows a typical image of the surface after it had been heated to 740 K. Analysis of this image shows that approximately 26% of the surface has been converted from (2×3) to (1×1). Examination of the (1×1) areas of Fig. 2 shows that all (1×1) areas contain at least one step edge. In fact, examination of all images taken during the course of this phase of the experiment showed that no single (1×1) area could be found which did not contain a step edge. This leads us to conclude that step edges serve as initial sites for the desorption process. What is also interesting is that (1×1) areas are present on both sides of a step edge, indicating that desorption occurs both backward from a step edge and forward from the base of a step. Table I shows the percentage area converted to (1×1) observed after each temperature treatment. Measurements were made after heating to 750 and 760 K; we were still able to observe some (2×3)N areas, but these areas were separated by much larger (1×1) areas, and we were thus prevented by the maximum scan size of the microscope (2000×2000

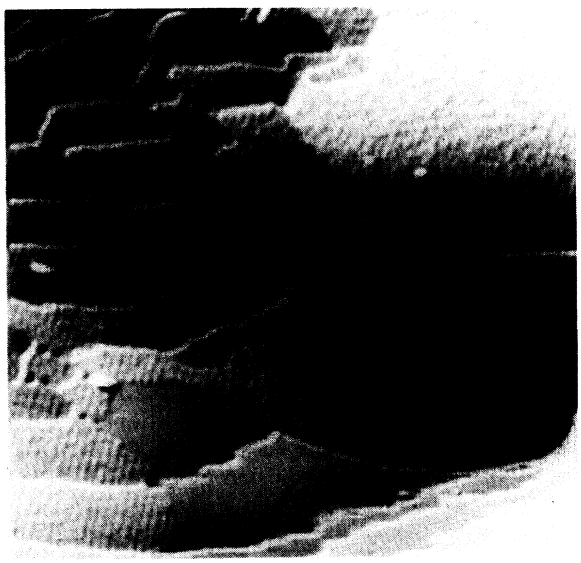

FIG. 2. 1000×1000 Å^2 image of the Cu{110}-(2×3)N surface after heating to 740 K. Approximately 26% of the surface has been converted to (1×1) (sample bias -1 V, $I=1$ nA).

TABLE I. Percentage of sample surface converted to (1×1) as a function of temperature.

T (K)	690	710	730	740
area (%)	1.6	3.0	22.4	37.7

Å^2) from determining how much of the (2×3)N reconstruction remained on the surface.

Figure 3 shows a boundary region between an area of the (2×3)N reconstruction and the clean Cu. At the top left-hand corner we see near-atomic resolution on the (1×1) Cu area. Although we were not able to resolve a corrugation in the [1$\bar{1}$0] direction, the 3.6-Å spacing of the corrugations in the [001] direction is consistent with the dimensions of the (1×1) unit cell. The boundary between the two regions is quite abrupt and lies along the [1$\bar{1}$0] direction. In the (2×3)N areas near the boundary, feature A is quite likely to be missing. Features B and C remain relatively intact. Much, if not all, of our insight into how desorption occurs on an atomic level occurs not as result of experimental observation but on the basis of theoretical simulation.[16] For example, Hood, Toby, and Weinberg[17] used a combined Monte Carlo simulation and continuum rate expression approach to describe molecular desorption of N_2 from a Ru{001} surface. Their simulated thermal-programmed desorption spectra agree well with the experimental results of Refs. 18 and 19. They demonstrated that a low-coverage peak in the desorption spectra was due to desorption of N_2, molecules located at the perimeter of N_2 islands and that the interior of the islands remains intact. Even though these simulations were carried out for the desorption of an adlayer, we see that the insights derived from that study are applicable to our study in that desorption observed in this system results in islands of clean Cu.

We discovered during attempts to perform scanning tunneling spectroscopy on this surface that we could remove the A feature from areas of the surface. Typically, this could be done by stabilizing the tip above the surface with tunneling conditions of 1 V and 1 nA, turning off the feedback, and then pulsing the voltage between 3 and 5 V. In Fig. 4(a), we see a 20×40 Å^2 area of the sample containing 12 A features. Figure 4(b) shows the same area after such a treatment; we see now only two A features. The remainder of the image, in which B features are now visible, resembles Fig. 1(a). It has been demonstrated that such treatments can result in atoms being removed from surfaces.[20] We view this as still further evidence for assigning feature A to be nitrogen derived. Attempts to induce desorption in this manner often resulted in degradation of resolution, possibly due to nitrogen adsorption onto the tunneling tip. It is known that even molecular nitrogen will adsorb dissociatively on tungsten at room temperatures.[21]

V. OXYGEN COADSORPTION RESULTS

The subsaturation nitrogen doses or the thermal treatments discussed earlier both resulted in areas of the clean (1×1) surface coexisting with areas of the α(2×3)N and β(2×3)N reconstructions respectively. Ideally one would like to observe the spatial relationship between the atoms in (1×1) and features in the (2×3) areas. We were not able to achieve atomic resolution on both the (1×1) and (2×3)N areas simultaneously. The best that we were able to achieve was the observation of corrugations in the [001] direction on an area of the clean surface

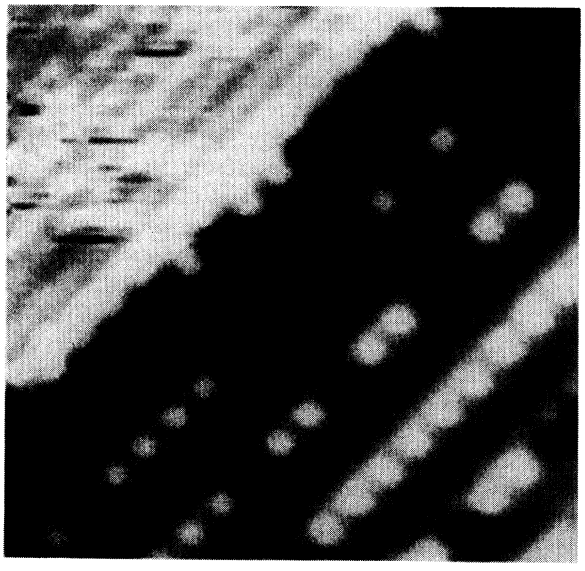

FIG. 3. 60×60 Å^2 image showing an area of clean Cu in the upper left-hand corner and the (2×3)N reconstruction. Away from the boundary the (2×3)N reconstruction is relatively intact. Along the boundary, feature A tends to be absent (sample bias −1 V, I=0.5 nA).

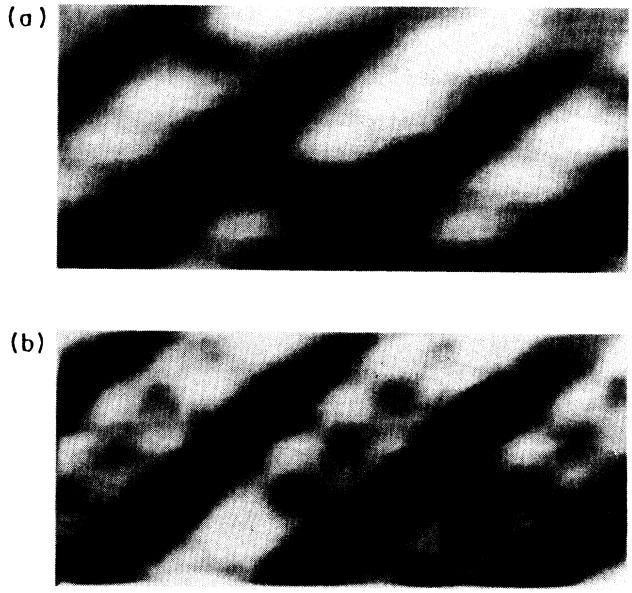

FIG. 4. 20×40 Å^2 images of the same area of the sample. (a) before and (b) after applying voltage pulses between the sample and the tip. These pulses resulted in the removal of 10 of the 12 A features visible in (a) (sample bias −1 V, I=1 nA).

bordering the $\beta(2\times3)$N as shown in Fig. 3. To obtain the spatial relationships between the (1×1) areas and the (2×3) areas, we chose to coadsorb oxygen on both these surfaces. Oxygen will adsorb dissociatively at room temperature on the Cu{110} surface and form a (2×1) reconstruction. Likewise, we can investigate the possibility of oxygen adsorption on the (2×3)N reconstructions.

The Cu{110}-(2×1)O surface has been extensively characterized by a large number of experimental techniques. Both the structure and mechanism of formation are known. This reconstruction was shown to be an added-row reconstruction consisting of strings of alternating Cu and O atoms aligned along the [001] direction of the substrate.[11–15] The oxygen atoms are adsorbed in subsurface long-bridge sites.[22]

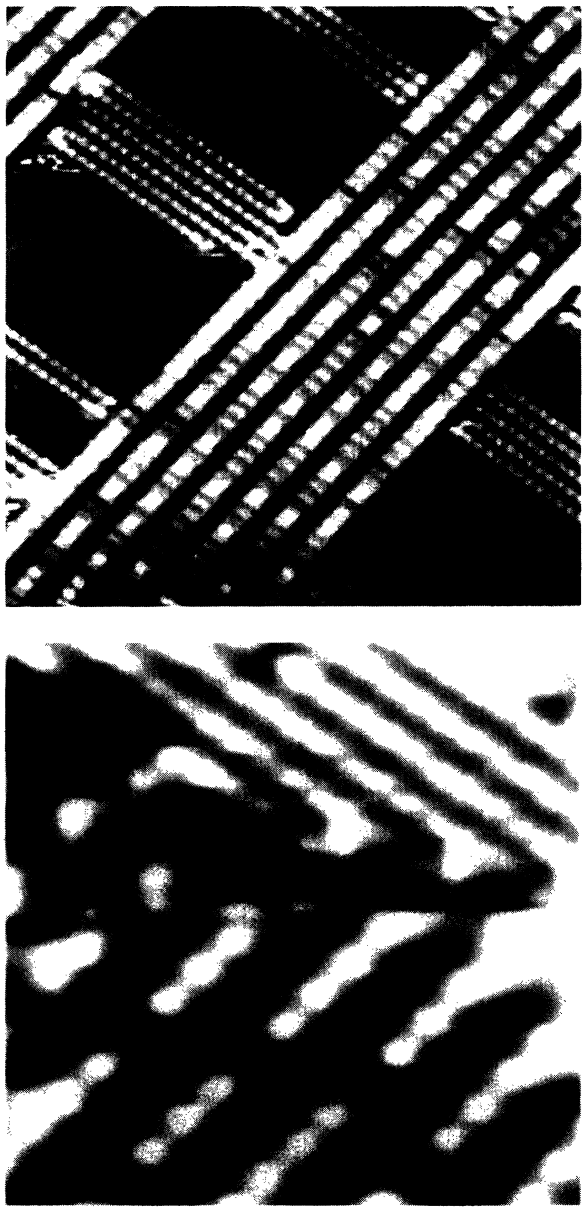

FIG. 5. Atomic-resolution images of codomains of the (2×1)O and (a) the $\alpha(2\times3)$N and (b) the $\beta(2\times3)$N reconstructions. (a) is a 200×200 Å^2 image taken with a sample bias of -2.5 V and a tunneling current of 1 nA. (b) is a 70×70 Å^2 image taken with a sample bias of -1.0 V and a tunneling current of 1 nA.

Because oxygen adsorbs dissociatively at room temperatures, we were able to dose oxygen onto the Cu{110} surface without removing it from the microscope. Figure 5(a) is a 200×200 Å^2 image with simultaneous atomic resolution on both the (2×1)O and $\alpha(2\times3)$N reconstructions. As observed in previous STM studies,[10–15] the Cu and O atoms order into islands with the long direction of the islands in the [001] directions of the substrate. The resultant surface with areas of both reconstructions occurring simultaneously takes on a "tartan"-like appearance. In this figure, we see that the Cu-O strings arbitrarily align themselves either with the *B* features or halfway between them. Figure 5(b) is a 70×70 Å^2 image with simultaneous atomic resolution on both the (2×1)O and $\beta(2\times3)$N reconstructions and shows the same spatial relationship between the unit cells for both reconstructions as observed in Fig. 5(a). The surface imaged in Fig. 5(b) was created by partially desorbing the (2×3)N reconstruction by heating the sample to 730 K and coadsorbing oxygen at room temperature to form the (2×1)O reconstruction in the resultant clean areas. We did not observe oxygen exposure to have any effect on the areas of either of the two (2×3)N reconstructions.

In the following section, we will use the spatial relationship between the atomic features observed in both reconstructions to help derive models for the (2×3)N reconstructions.

VI. STRUCTURAL MODELS

In general, building models for surface reconstructions based on STM data is somewhat speculative. A scanning-tunneling-microscopy image represents a convolution of local atomic and electronic structure of both the sample and the tunneling tip. This can easily be seen in Fig. 6 where a change in the tunneling tip causes drastic changes in a STM image of codomains of the $\alpha(2\times3)$N, (2×1)O, and clean surface. In one part of the image the areas of the (2×3)N and (2×1)O reconstructions appear as depressions relative to the clean surface. This behavior has been observed before and has been attributed to oxygen adsorption on the tip itself.[13] We also believe that this is the case as we only observed such drastic changes in images of the (2×3)N reconstructions when we were performing experiments that involved oxygen coadsorption. A further disadvantage of STM is the lack of chemical sensitivity; when one views a STM image of a surface with a variety of different atomic species present, it is often difficult to make elemental assignments to the observed atomic-scale features. In the several STM studies of the Cu{110}-(2×1)O (Refs. 11–15) and Cu{100}-$(2\sqrt{2}\times\sqrt{2})R45°$-O (Ref. 23) systems, in only a few cases do authors attempt to make elemental assignments of the features observed in their images;[13,15] most simply refer to the features observed in their images as Cu-O bonds. In Refs. 13 and 15 the protrusions observed in the (2×1) unit cells are assigned to the Cu atoms. Fi-

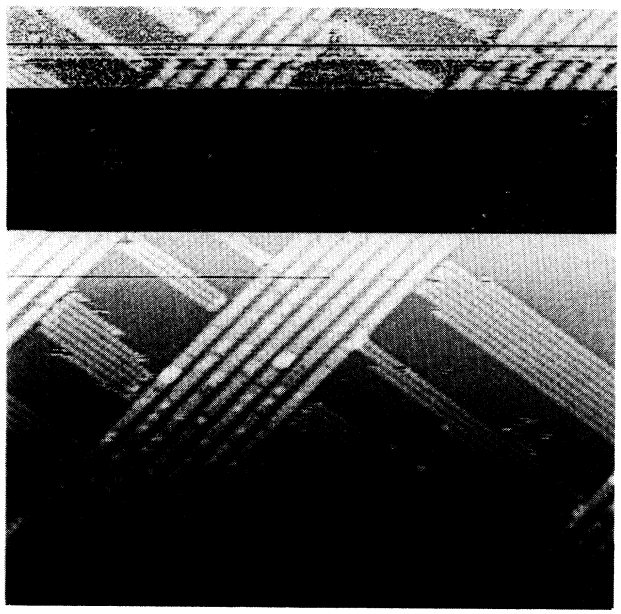

FIG. 6. 400×400 Å^2 image of codomains of the (2×1)O and α(2×3)N reconstructions taken with a sample bias of −2.5 V and a tunneling current of 1 nA. The image shows the effects of multiple tip changes that occurred occasionally while performing oxygen adsorption experiments.

nally, STM is an extremely surface-sensitive technique; hence, it is often impossible to obtain information on how the atomic-scale features viewed in an image are related to the atoms in the layers below.

Let us examine how images like that of Fig. 7(a) help us to circumvent the above limitations of STM. The Cu{110}-(2×1)O reconstruction is a well-understood surface reconstruction consisting of added rows of alternating Cu and O atoms running in the [001] directions.[12–15] The Cu atoms in the rows are in twofold-hollow sites above the surface and the O atoms are in long-bridge sites bonded slightly below the neighboring Cu atoms.[22] The spatial relationship of the atoms in the (2×1)O reconstruction to those in the layers below is well understood and hence can be used to derive the relationship between the atomic features observed in the (2×3)N reconstruction and the atoms in the subsurface layers. Figures 7(b)–7(e) shows a series of possible atomic relationships based on Fig. 7(a) and a set of explicit assumptions. Figure 7(b) shows the spatial relationship between the *A* and *B* features of the (2×3)N surface as observed in Fig. 7(a) and the substrate atoms below, based on the assumptions that we are imaging the Cu atoms in the (2×1) reconstruction and that the *B* features are roughly coplanar with the added rows of the (2×1) reconstruction. Figure 7(c) assumes that we are imaging the O atoms in the (2×1) reconstruction and that the *B* features are roughly coplanar with the added rows. Figure 7(d) assumes that we are imaging the Cu atoms of the (2×1), but assumes that the *B* features are roughly coplanar with the first layer of substrate atoms. Figure 7(e) assumes that we are imaging the O atoms within the (2×1) reconstruction and that the *B* features are roughly coplanar with the first layer of substrate atoms.

Thoughtful examination of these possible arrangements, eliminates those shown in Figs. 7(c) and 7(d) from further consideration. The arrangement shown in Fig. 7(c) and Fig. 7(d) place the *B* features in either short-bridge sites or atop sites, respectively; it is highly unlikely that a Cu or N atom would reside in such a site. Although Fig. 7(e) places the *B* features in a long-bridge site, which is certainly a reasonable position if the *B* features were nitrogen derived, it places the *A* features in the awkward position of being in an atop site. We believe that the preceding sections of this paper present strong evidence for assigning feature *A* to be nitrogen derived. Hence, we do not view the arrangement shown in Fig. 7(e) as a possible atomic arrangement.

We are left with Fig. 7(b), on the basis of which we will offer models for both the (2×3)N reconstructions. The arrangement shown in Fig. 7(b) is quite reasonable, based a number of considerations. It assumes that the Cu atoms are viewed in the (2×1)O reconstruction, which is in agreement with the elemental assignments in Refs. 13 and 15. The assumption that the *B* features are roughly coplanar with the atoms in the added rows places them in twofold-hollow sites, which would be reasonable sites for Cu atoms. We will assume, therefore, that the *B* features are copper derived. We note that careful measurements of positions of the *C* features observed in Figs. 1(a) and 1(b) relative to the *B* and *A* features places the *C* features in long-bridge sites relative to the substrate layer.

In order to construct models for the observed reconstructions, it is necessary to have an accurate knowledge of the number of nitrogen atoms per (2×3) unit cell. Baddorf and Zehner[2] report a coverage of $\frac{2}{3}$ of a monolayer based on XPS, and hence with this coverage there should be four nitrogen atoms per unit cell. References 6 and 7 report a coverage of 0.2±0.05 ML and propose models based on one nitrogen atom per unit cell. We note that a study of activated nitrogen adsorption on the {210} surfaces of Cu and Ni resulted in {110} facets that displayed (2×3) LEED patterns; the nitrogen coverage measured via AES in this study for both the Cu and Ni surfaces was reported to be 0.65 ML.[24] A study of the Ni{110}-(2×3)N surface also used AES and derived a nitrogen coverage of 0.5 ML.[25] The higher coverage value of Baddorf and Zehner[2] is more consistent with those values previously reported in the literature. Since the sample preparation methods employed in this study to produce the β(2×3)N reconstruction closely resemble the method they used to prepare a nitrogen-saturated (2×3) surface, we will construct a model for this reconstruction based on their reported coverage of $\frac{2}{3}$ of a monolayer. Since the only observed difference in the STM images between the α(2×3)N and β(2×3)N reconstructions is the occupancy of the *A* sites [maximum of one per (2×3) unit cell], we will construct a model for the α(2×3)N reconstruction that assumes a coverage of $\frac{1}{2}$ of a monolayer. These models are shown in Fig. 8.

These models consist of two added rows of copper atoms in the [1$\bar{1}$0] direction for every three rows of the substrate. To accommodate the $\frac{2}{3}$-MLN coverage report-

ed in Ref. 2, in the model for the $\beta(2\times3)$N reconstruction [Fig. 8(a)], we have placed an array of N atoms in alternating subsurface and supersurface long-bridge sites bonded to the Cu atoms within added rows, and another alternating array of N atoms bonded to the substrate atoms between the rows. For the $\alpha(2\times3)$N reconstruction [Fig. 8(b)], we assume a model where the supersurface N atoms bonded within the added rows have been removed. These models associate the *A* features with N atoms bonded in long-bridge sites above the Cu atoms of the added rows. Because of both the position of the *B* features and their similarity within the images to the Cu

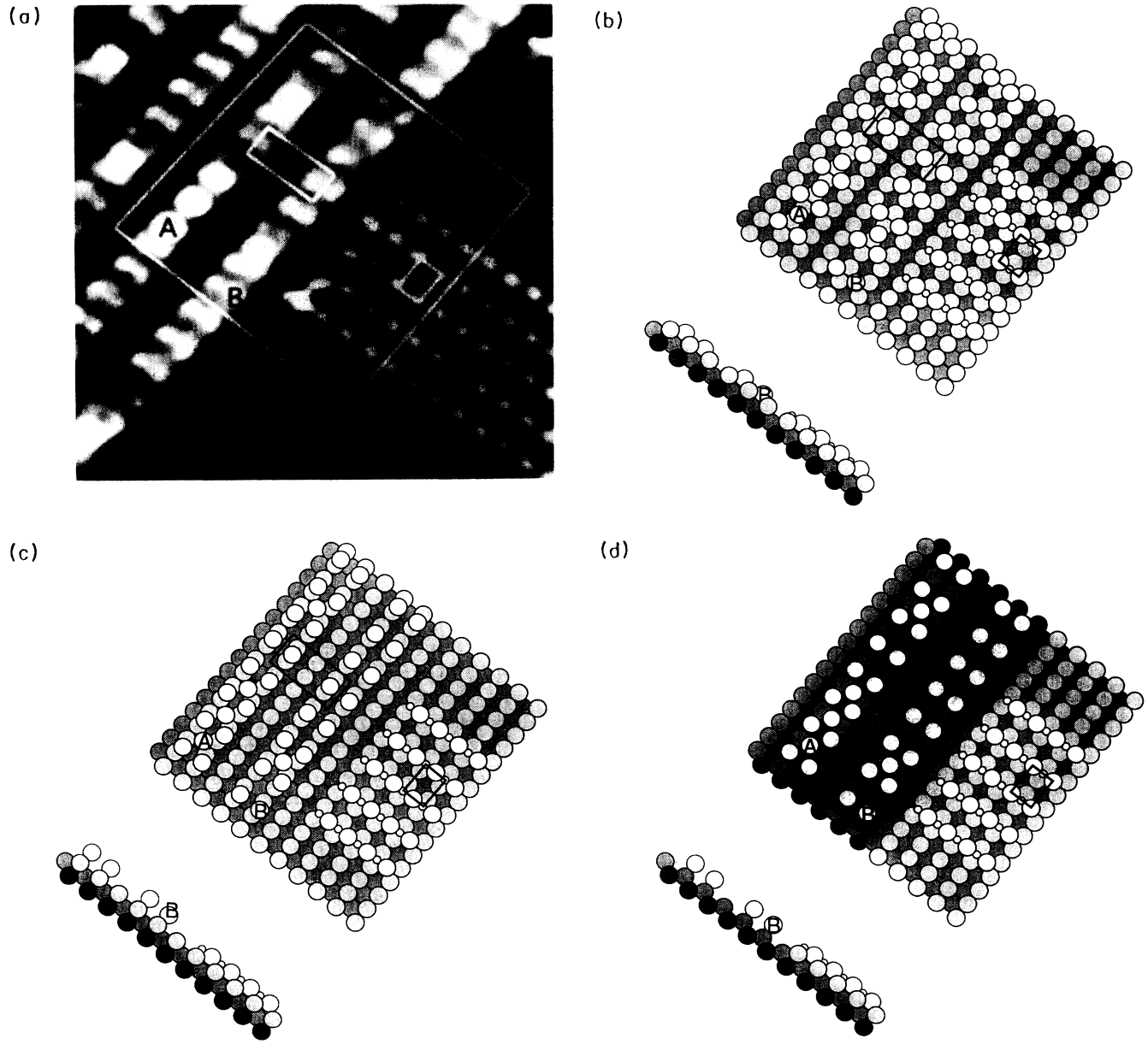

FIG. 7. (a) 70×70 Å^2 section of Fig. 6(a) with the contrast enhanced to help locate the atomic positions in the $\alpha(2\times3)$N reconstruction relative to the (2×1)O reconstruction. (2×3) and (2×1) unit cells are outlined and individual *A* and *B* features are indicated. (b)–(e) ball models (side and top views) for the features observed in the two reconstructions based on the area contained within the large square in (a). Shaded circles represent substrate Cu atoms, large open circles represent added-row Cu atoms and *A* and *B* features, small open circles represent O atoms. (b) assumes that Cu atoms are viewed within the (2×1) area and that the *B* features are roughly coplanar with the added Cu-O rows. (c) assumes that oxygen atoms are viewed with the (2×1) area and that the *B* features are roughly coplanar with the added rows. (d) assumes that Cu atoms are viewed within the (2×1) area and that the *B* features are roughly coplanar with the first layer of the substrate. (e) assumes that oxygen atoms are viewed within the (2×1) area and that the *B* features are roughly coplanar with the added row. After careful consideration, (b) appears to the most satisfying option.

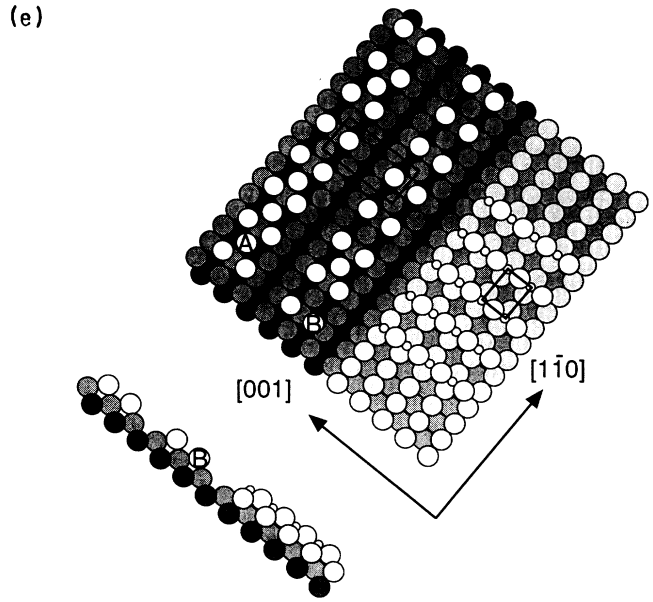

FIG. 7. (*Continued*).

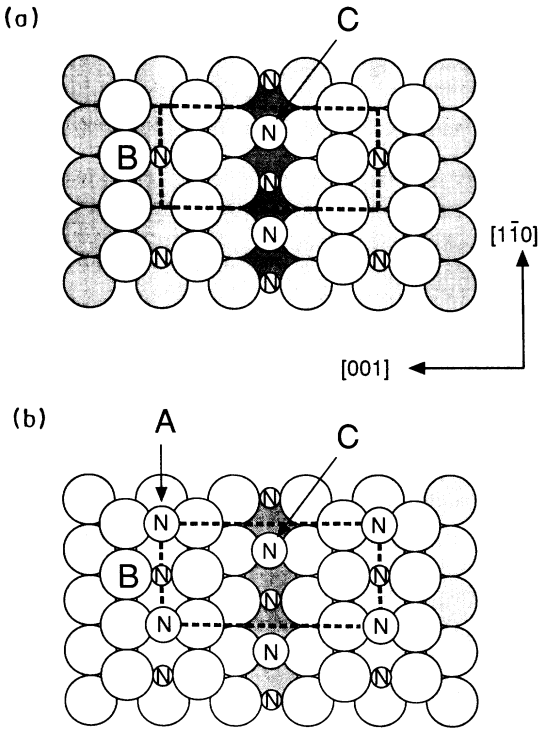

FIG. 8. Models for the (2×3)N reconstructions based on this work. (a) β(2×3)N reconstruction and (b) α(2×3) reconstruction. These are double-added-row models, where the *A* features are associated with N atoms in supersurface long-bridge sites in the added Cu rows. *B* features are associated with Cu atoms in the added rows but bonded to N atoms in subsurface long-bridge sites. *C* features are associated with N atoms bonded in supersurface long-bridge sites to the Cu atoms of the first layer of the substrate. We assume also that there are N atoms bonded in subsurface long-bridge sites to atoms in the first layer of the substrate. These models have nitrogen coverages of $\frac{2}{3}$ and $\frac{1}{2}$ ML respectively.

atoms of the (2×1)O reconstruction, we associate the pairs of *B* features with Cu atoms that have a N atom bonded in a subsurface long-bridge site between them. Because of the position of the *C* features, we have chosen to associate them with N atoms bonded in a supersurface long-bridge site to the Cu atoms of the substrate. To accommodate the $\frac{2}{3}$-ML N coverage requirement and for reasons of symmetry, we have assumed the existence of another N atom bonded in a subsurface long-bridge site within the first layer of the substrate.

VII. DISCUSSION

The models presented in Fig. 8 are in agreement with many aspects of the previous work done on this system; although these models use higher N coverages than that reported in Refs. 6 and 7, they agree with the positioning of Cu atoms in those studies. We note that Ref. 6 was on ion-scattering study, which is highly sensitive to the positions of the Cu atoms but relatively insensitive to the positions of the nitrogen atoms. Alternating arrays of subsurface and supersurface nitrogen atoms were postulated by Baddorf and Zehner to account for the $\frac{2}{3}$-ML coverage in the absence of a surface reconstruction.[2] The models presented here have N atoms placed only in a single type of adsorption site, in agreement with the XPS lineshape analysis done in Ref. 2. These adsorption sites are long-bridge sites in agreement with HREELS measurements for both the Cu{110}-(2×3)N and Ni{110}-(2×3)N systems.[1,25] To discuss our results in light of the photoelectron-diffraction study of Ref. 3 and ion-scattering study of Ref. 4, we note that the pseudosquare reconstruction model was proposed largely on the evidence of the latter ion-scattering study. From the sample preparation method, it seems likely that the surface studied was the high-coverage β(2×3) reconstruction. The lattice parameters determined in Ref. 4 are from a consideration of the value of the surface threshold grazing-incidence angle compared to that of the clean surface. No change was found in the Cu-Cu lattice spacing in the ⟨110⟩ azimuth, which is consistent with both missing-row and pseudosquare models. In ⟨111⟩, ⟨211⟩, and ⟨100⟩ azimuths, a more complex behavior is observed, with the distinct possibility that the threshold grazing-incidence angle observed consists of contributions from more than one value of the Cu-Cu lattice spacing. In the added-row models of Fig. 8, there are two different Cu-Cu lattice spacings present in equal proportions. One is equivalent to the lattice spacing of the clean surface, and the other is twice this value. A value of 6.4±0.3 Å is calculated in Ref. 4 for the Cu-Cu spacing in the ⟨211⟩ azimuth. On the basis of the added-row models shown in Fig. 8, we expect lattice parameters of approximately 4.4 and 8.8 Å, and hence a mean value of 6.6 Å. The difficulty in making an unambiguous structure determination, especially given a complex surface reconstruction, using the grazing-angle method cannot be overestimated. Finally, in relation to the LEED *I-V* analysis done in Ref. 9, we note that the models presented in Fig. 8, neither conflict with nor confirmed by this study, in that LEED *I-V* curves were not calculated for the atomic ar-

rangements contained within these models.

As mentioned earlier, the models we have derived for the (2×3)N-induced reconstructions involve added rows of Cu atoms, whereas the ion scattering produced a missing-row model. Now, from a structural point of view, there is no difference between the two. However, there are differences in the formation of the two structures. STM studies of the dynamics of the formation of the Cu{110}-(2×1)O reconstruction show that it is an added-row structure formed by Cu atoms diffusing from step edges.[12–15] Similarly the Cu{100}-$(2\sqrt{2}\times\sqrt{2})R45°$-O reconstruction was shown by a STM study to form via a missing-row mechanism, by observing the ejection of Cu atoms and subsequent expansion of nearby step edges.[23] Although, without a STM capable of operating at high temperatures, we cannot watch the (2×3)N reconstruction form, the structural model derived in this study and the spatial relationship between the codomains of the (2×1)O and $\alpha(2\times3)$N reconstructions as shown in Fig. 7(a), imply that the method of formation of the (2×3)N reconstruction involves added rows of Cu atoms running in the $[1\bar{1}0]$ direction.

A double-added-row model for the $(2\times3)N$ reconstructions is perhaps the most paradoxical result of our study, in that both N and O adsorb in long-bridge sites on the Cu{110} surface, both induce added-row reconstructions, both reconstructions exhibit highly directional island growth, and yet the island growth directions are perpendicular. We must, therefore, infer from this that the preferential direction of island growth is determined by interactions occurring during the formation of the reconstruction rather than by adsorption geometry. As has been observed in all the STM studies of the (2×1)O reconstruction, there is a weaker attractive interaction along the $[1\bar{1}0]$ direction which is responsible for slow island growth in this direction at low O coverages and for the removal of antiphase boundaries at higher coverages.[11–15] Since the nitrogen reconstruction does not involve alternating strings of N and Cu atoms like the (2×1)O reconstruction, perhaps it is then a similar attractive interaction along the $[1\bar{1}0]$ direction which dominates during the formation of the (2×3)N reconstruction.

It seems reasonable to ask why there are both α and β (2×3)N reconstructions. The work of Baddorf and Zehner[2] may provide a possible explanation. After 200-eV nitrogen doses at 300 K, they observed the nitrogen coverages to saturate near 1 ML. The width of the N 1s core indicated that only one site was occupied for coverages below $\frac{2}{3}$ ML, but additional site(s) were occupied at higher coverages. Perhaps, upon annealing to 600 K, it is the nitrogen atoms which are adsorbed in these additional site(s) that become the A features observed in this study. Regarding these A features, their assignment as nitrogen atoms and as being adsorbed in supersurface long-bridge sites in the added rows, would make them experience a much stronger electric field while the tip was scanned over the surface. It is not surprising therefore that these A features might undergo tip-induced desorption.

Finally, in our discussion, we recall that the 500-eV bombardment was more efficient in the production of A features than that at 200 eV. In the case of Cu{100} a nitrogen-induced $c(2\times2)$ reconstruction could be achieved alternatively through bombardment of activated nitrogen[26] or by cooling the sample to 100 K and dosing with ammonia and then heating to drive off the hydrogen.[27] In view of the dependency on the ion energy, it seems interesting to speculate whether both, or only one of the (2×3) reconstructions could be created through ammonia dehydrogenation.

VIII. CONCLUSIONS

We have used scanning tunneling microscopy to investigate surface structures arising from the bombardment of activated nitrogen onto the Cu{110} surface followed by annealing. We have varied the nitrogen dose and found that for very low doses, images of the annealed surface show that the (2×3)N reconstruction forms in rectangular islands elongated in the $[1\bar{1}0]$ direction. Increasing the nitrogen dose resulted in the gradual appearance of an additional N-induced structure also possessing a (2×3) periodicity. We have examined these structures for a variety of nitrogen doses, beam energies, imaging conditions, and annealing temperatures and conclude that there exist both low- and high-nitrogen-coverage (2×3) reconstructions, which we label as the $\alpha(2\times3)$N and $\beta(2\times3)$N reconstructions, respectively. Oxygen coadsorption studies support added-row models for both reconstructions. We have devised models based on pairs of added $\langle 110\rangle$ rows of Cu atoms and on N adsorbed in long-bridge sites with N coverages of $\frac{1}{2}$ and $\frac{2}{3}$ ML for the two reconstructions. Images of the surface before and after heating to temperatures at which partial desorption of the $\beta(2\times3)$N reconstruction occurred show that thermal desorption results in islands of clean Cu centered on step edges. Pulsing the voltage between the sample and tunneling tip was also found to induce desorption of only those nitrogen atoms adsorbed in supersurface bridge sites within the added rows.

ACKNOWLEDGMENTS

We would like to thank M. Bowker for the use of his Cu{110} crystal. We would also like to thank P. W. Murray, P. Harrison, G. Dickenson, P. Unsworth, and A. Ellis for technical assistance during various phases of these experiments.

*Present address: Physics Dept., University of Warwick, Coventry CV4 7AL, United Kingdom.

[1]D. Heskett, A. Baddorf, and E. W. Plummer, Surf. Sci. **195**, 94 (1988).

[2]A. P. Baddorf and D. M. Zehner, Surf. Sci. **238**, 255 (1990).

[3]A. W. Robinson, D. P. Woodruff, J. S. Somers, A. L. D. Kil-

coyne, D. E. Ricken, and A. M. Bradshaw, Surf. Sci. **237**, 99 (1990).

[4]M. J. Ashwin and D. P. Woodruff, Surf. Sci. **237**, 108 (1990).

[5]M. J. Ashwin, D. P. Woodruff, A. L. D. Kilcoyne, A. W. Robinson, J. S. Somers, D. E. Ricken, and A. M. Bradshaw, J. Vac. Technol. A **9**, 1856 (1991). We recently became aware of a recent x-ray scattering study that lends support to a modified pseudosquare model, see A. P. Baddorf, D. M. Zehner, G. Helgesen, D. Gibbs, A. R. Sandy, and S. G. J. Mochrie, Phys. Rev. B **48**, 9013 (1993).

[6]R. Spitzl, H. Niehus, and G. Comsa, Surf. Sci. Lett. **250**, L355 (1991).

[7]H. Niehus, R. Spitzl, K. Besocke, and G. Comsa, Phys. Rev. B **43**, 12 619 (1991).

[8]F. M. Leibsle, R. Davis, and A. W. Robinson, Phys. Rev. B **47**, 10 052 (1993).

[9]D. T. Vu Grimsby, M. Y. Zhou, and K. A. R. Mitchell, Surf. Sci. **271**, 519 (1992).

[10]F. M. Chua, Y. Kuk, and P. J. Silverman, Phys. Rev. Lett. **63**, 386 (1989).

[11]D. J. Coulman, J. Wintterlin, R. J. Behm, and G. Ertl, Phys. Rev. Lett. **64**, 1761 (1990).

[12]F. Jensen, F. Besenbacher, E. Laegsgaard, and I. Stensgaard, Phys. Rev. B **41**, 10 233 (1990).

[13]Y. Kuk, F. M. Chua, P. J. Silverman, and J. A. Meyer, Phys. Rev. B **41**, 12 393 (1990).

[14]J. Wintterlin, R. Schuster, D. J. Coulman, G. Ertl, and R. J. Behm, J. Vac. Sci. Technol. B **9**, 902 (1991).

[15]F. M. Chua, Y. Kuk, and P. J. Silverman, J. Vac. Sci. Technol. A **8**, 305 (1990).

[16]See, for example, S. J. Lombardo and A. T. Bell, Surf. Sci. Rep. **13**, 1 (1991).

[17]E. S. Hood, B. H. Toby, and W. H. Weinberg, Phys. Rev. Lett. **55**, 2437 (1985).

[18]P. Feulner and D. Menzel, Phys. Rev. B **25**, 4295 (1982).

[19]D. Menzel, H. Pfnür, and P. Feulner, Surf. Sci. **126**, 374 (1983).

[20]I.-W. Lyo and Ph. Avouris, Science **253**, 173 (1991).

[21]See, for example, K. Griffiths, C. Kendon, D. A. King, and J. B. Pendry, Phys. Rev. Lett. **46**, 1584 (1981).

[22]H. Dürr, Th. Fauster, and R. Schneider, Surf. Sci. **244**, 237 (1991).

[23]F. Jensen, F. Besenbacher, E. Laegsgaard, and I. Stensgaard, Phys. Rev. B **42**, 9206 (1990).

[24]R. E. Kirby, C. S. McKee, and L. V. Renny, Surf. Sci. **97**, 457 (1980).

[25]E. Roman and R. Riwan, Surf. Sci. **118**, 682 (1982).

[26]H. C. Zeng, R. N. S. Sodhi, and K. A. R. Mitchell, Surf. Sci. **188**, 599 (1987).

[27]R. Franchy, M. Wutting, and H. Ibach, Z. Phys. B **64**, 453 (1986).

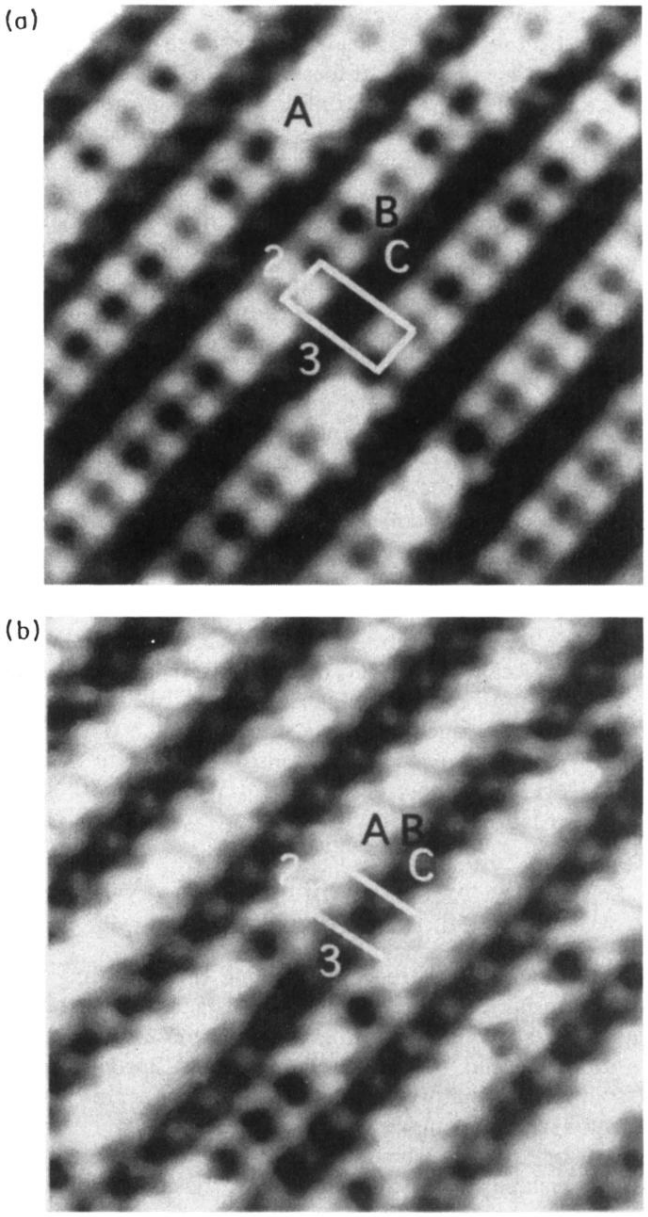

FIG. 1. (a) 60×60 Å^2 STM image of a typical area of the Cu{110} surface following a 200-eV 150-μC, N-ion bombardment and annealing to 600 K. (Sample bias -1.0 V, $I=1$ nA.) (b) 60×60 Å^2 STM image of a typical area of the Cu{110} surface following a 500-eV, 4400-μC, N-ion bombardment and annealing to 600 K. (Sample bias 0.06 V, $I=1$ nA.) Atomic-scale features observed in these images are labeled *A*, *B*, and *C*. (2×3) unit cells are outlined. The only difference between the two images appears to be the increase in density of the *A* features.

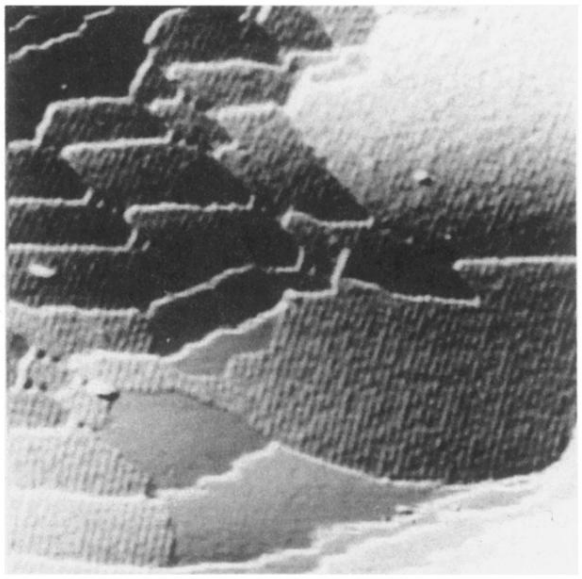

FIG. 2. 1000×1000 Å^2 image of the Cu{110}-(2×3)N surface after heating to 740 K. Approximately 26% of the surface has been converted to (1×1) (sample bias -1 V, $I = 1$ nA).

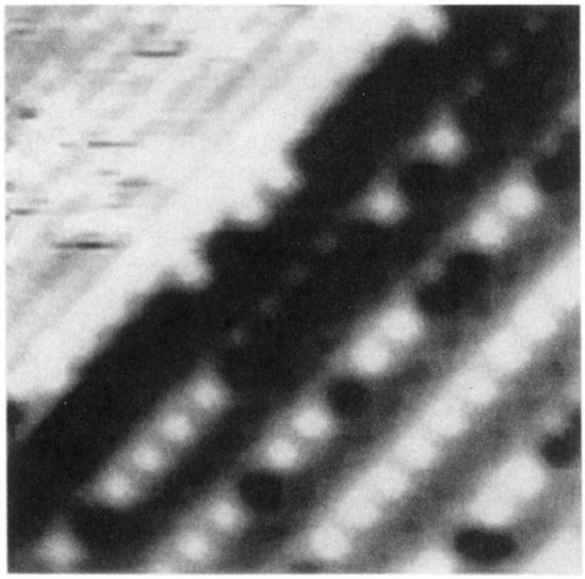

FIG. 3. 60×60 Å^2 image showing an area of clean Cu in the upper left-hand corner and the (2×3)N reconstruction. Away from the boundary the (2×3)N reconstruction is relatively intact. Along the boundary, feature *A* tends to be absent (sample bias -1 V, $I=0.5$ nA).

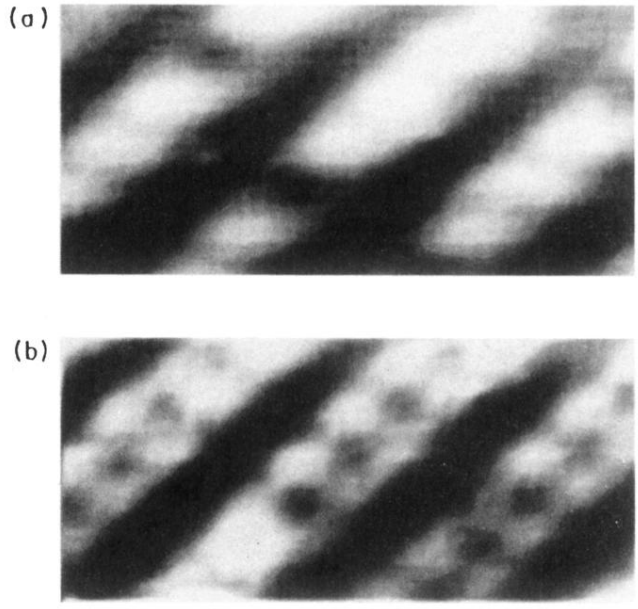

FIG. 4. 20×40 Å^2 images of the same area of the sample. (a) before and (b) after applying voltage pulses between the sample and the tip. These pulses resulted in the removal of 10 of the 12 *A* features visible in (a) (sample bias -1 V, $I=1$ nA).

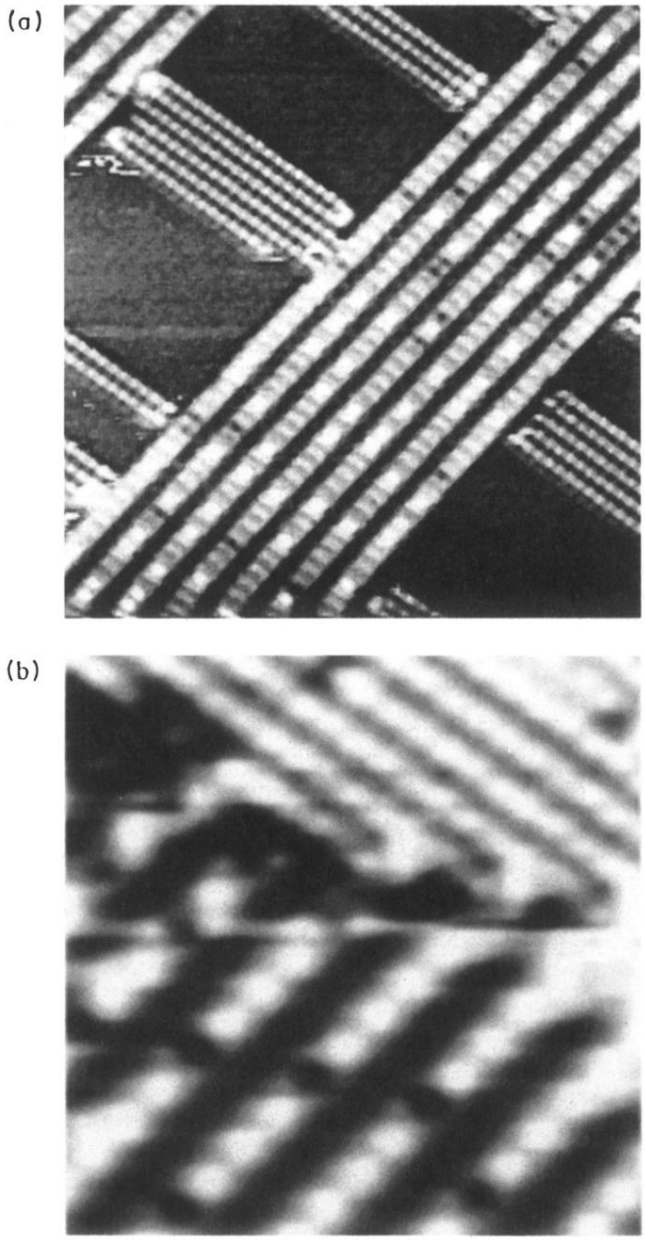

FIG. 5. Atomic-resolution images of codomains of the (2×1)O and (a) the $\alpha(2\times3)$N and (b) the $\beta(2\times3)$N reconstructions. (a) is a 200×200 Å^2 image taken with a sample bias of -2.5 V and a tunneling current of 1 nA. (b) is a 70×70 Å^2 image taken with a sample bias of -1.0 V and a tunneling current of 1 nA.

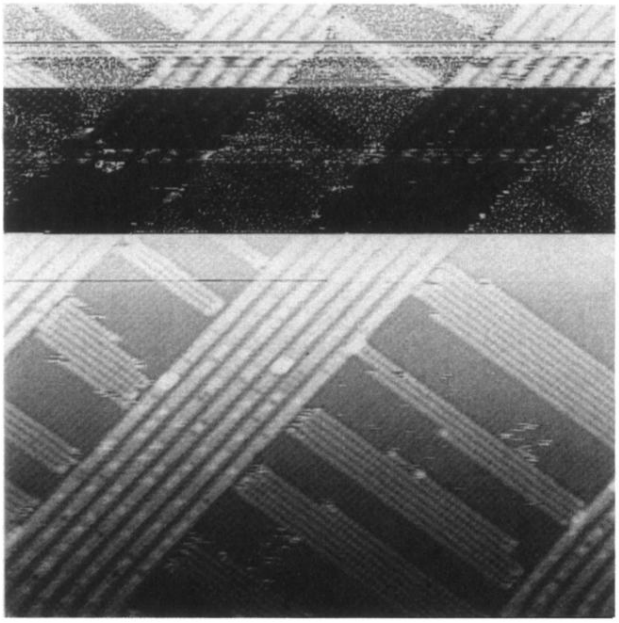

FIG. 6. 400×400 Å^2 image of codomains of the (2×1)O and $\alpha(2\times3)$N reconstructions taken with a sample bias of -2.5 V and a tunneling current of 1 nA. The image shows the effects of multiple tip changes that occurred occasionally while performing oxygen adsorption experiments.

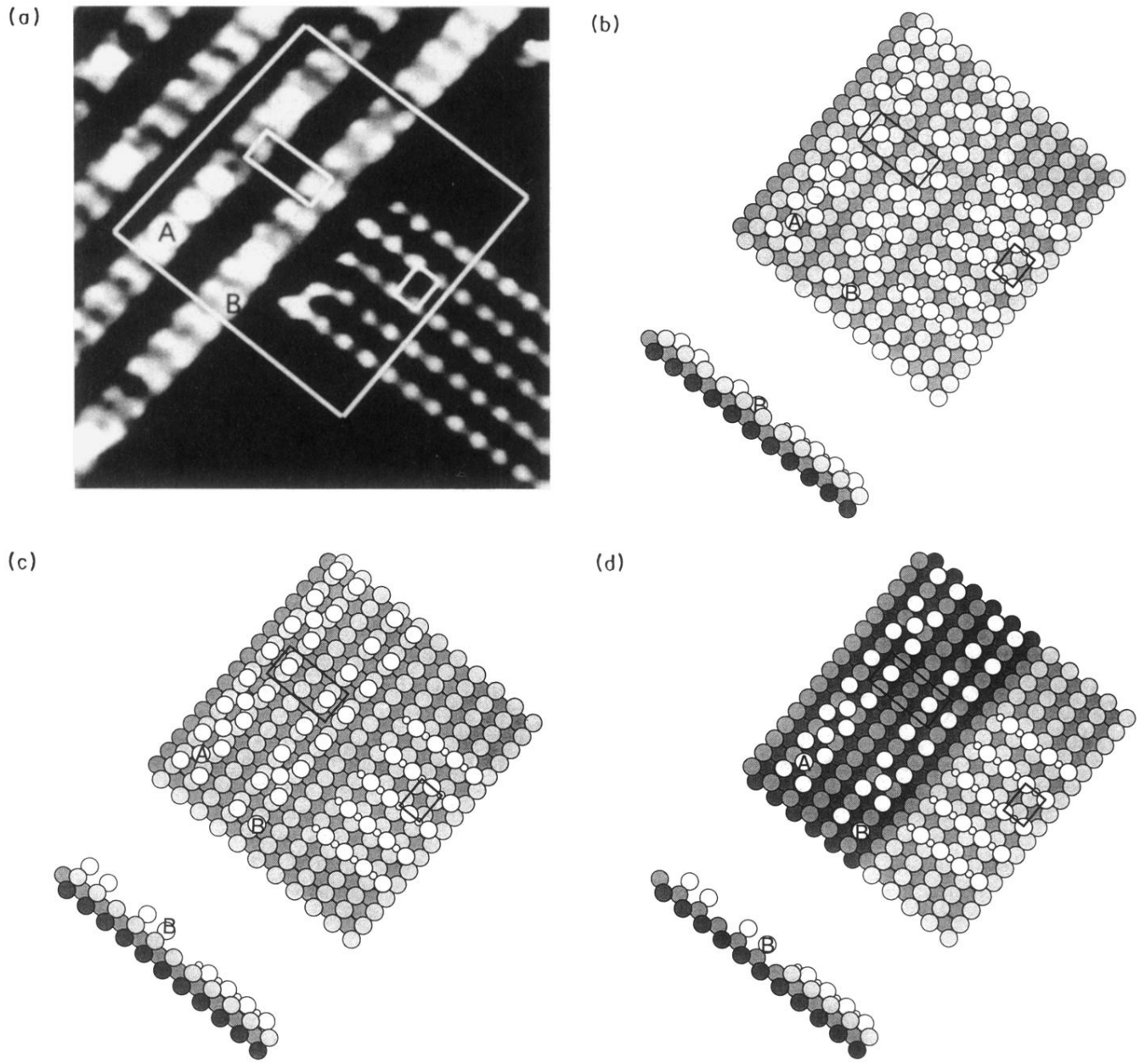

FIG. 7. (a) 70×70 Å^2 section of Fig. 6(a) with the contrast enhanced to help locate the atomic positions in the $\alpha(2\times3)$N reconstruction relative to the (2×1)O reconstruction. (2×3) and (2×1) unit cells are outlined and individual *A* and *B* features are indicated. (b)–(e) ball models (side and top views) for the features observed in the two reconstructions based on the area contained within the large square in (a). Shaded circles represent substrate Cu atoms, large open circles represent added-row Cu atoms and *A* and *B* features, small open circles represent O atoms. (b) assumes that Cu atoms are viewed within the (2×1) area and that the *B* features are roughly coplanar with the added Cu-O rows. (c) assumes that oxygen atoms are viewed with the (2×1) area and that the *B* features are roughly coplanar with the added rows. (d) assumes that Cu atoms are viewed within the (2×1) area and that the *B* features are roughly coplanar with the first layer of the substrate. (e) assumes that oxygen atoms are viewed within the (2×1) area and that the *B* features are roughly coplanar with the added row. After careful consideration, (b) appears to the most satisfying option.

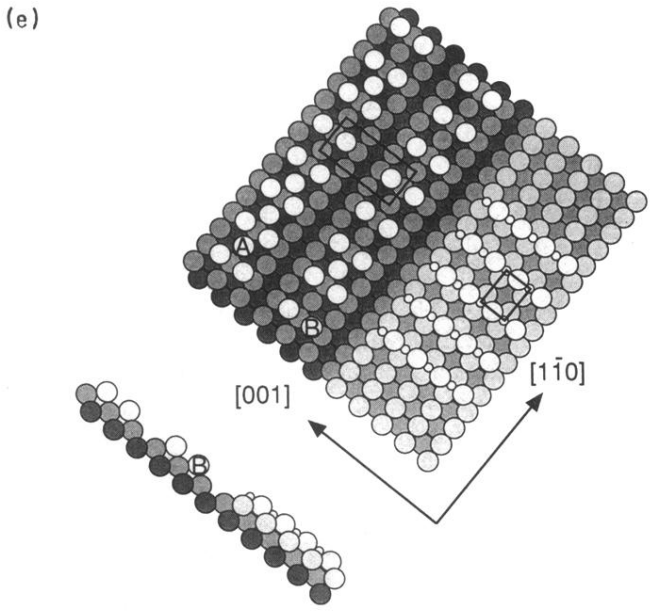

FIG. 7. (*Continued*).

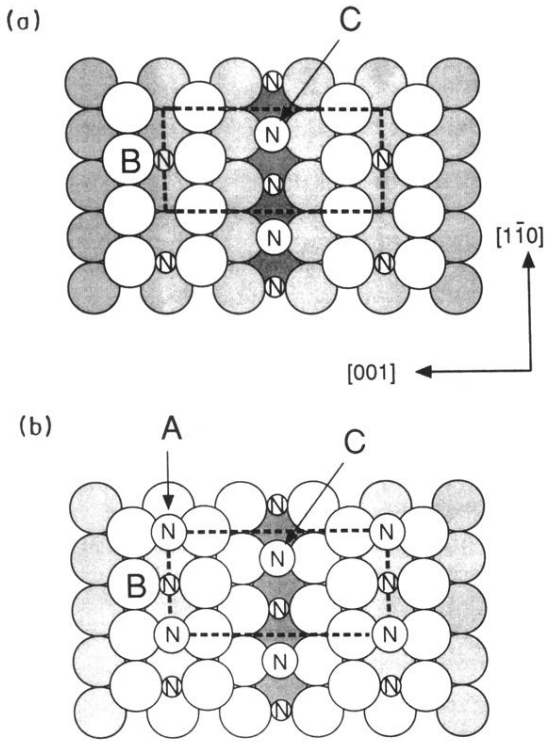

FIG. 8. Models for the (2×3)N reconstructions based on this work. (a) $\beta(2\times3)$N reconstruction and (b) $\alpha(2\times3)$ reconstruction. These are double-added-row models, where the *A* features are associated with N atoms in supersurface long-bridge sites in the added Cu rows. *B* features are associated with Cu atoms in the added rows but bonded to N atoms in subsurface long-bridge sites. *C* features are associated with N atoms bonded in supersurface long-bridge sites to the Cu atoms of the first layer of the substrate. We assume also that there are N atoms bonded in subsurface long-bridge sites to atoms in the first layer of the substrate. These models have nitrogen coverages of $\frac{2}{3}$ and $\frac{1}{2}$ ML respectively.